Atmospheric Research 182 (2016) 87–101

Contents lists available at ScienceDirect

Atmospheric Research

journal homepage: www.elsevier.com/locate/atmosres

Stable isotope composition of precipitation in the south and north slopes of Wushaoling Mountain, northwestern China

Li Zongxing [a,b,*], Feng Qi [a], Yong Song [b], Q.J. Wang [b], Jiao Yang [c], Li Yongge [a], Li Jianguo [a], Guo Xiaoyan [a]

[a] Key Laboratory of Ecohydrology of Inland River Basin/Gansu Hydrology and Water Resources Engineering Research Center, Cold and Arid Region Environment and Engineering Research Institute, Chinese Academy of Sciences, Lanzhou 730000, China
[b] CSIRO Land and Water, Private Bag 10, Clayton South, VIC 3169, Australia
[c] Key Laboratory of Meteorological Disaster, Ministry of Education/Institute of Climate Change and Evaluation between China and UK, Nanjing University of Information Science and Technology, Nanjing 210044, China

ARTICLE INFO

Article history:
Received 31 March 2016
Received in revised form 15 July 2016
Accepted 20 July 2016
Available online 25 July 2016

Keywords:
Stable isotope
Temperature
Altitude
Moisture sources
Qilian Mountains

ABSTRACT

A study of spatial and temporal variability of precipitation isotope composition on the southern and north slopes of Wushaoling Mountain was conducted in order to explore the processes influencing its evolution. The analysis indicated that the isotopic composition, the slopes and intercepts of Local Meteroic Water Lines, altitude gradients and temperature effect are higher on the north slope than those on the south slope. The *d*-excess showed an increase from lower to higher altitudes, and the altitude gradients changed with season. The correlation coefficients between $\delta^{18}O$ and *d*-excess decreased with increasing altitude due to weakening sub-cloud evaporation. Westerly wind principally dominates Wushaoling Mountain, so the relatively negative stable isotope values observed are related to the long distance transportation of water vapor in spring and winter. In summer and autumn, the locally strong sub-cloud evaporation cause relatively higher $\delta^{18}O$ and lower *d*-excess. The results suggested that the sub-cloud evaporation has enriched the $\delta^{18}O$ composition by 23%, 23%, 32%, 42% and 29% in May, June, July, August and September, respectively. In some circumstances, $\delta^{18}O$ and δD were depleted at the end of multi-days rainfall events due to the rainout process. In addition, monsoonal moisture caused some negative $\delta^{18}O$ in summer when an enhanced cyclonic circulation had developed on Tibetan Plateau. The study enhances the knowledge of isotopic evolution of precipitation and provides a basis for further study of isotopic hydrology in arid regions.

1. Introduction

The $\delta^{18}O$ and δD of meteoric waters have been widely used in hydrologic and climatic studies, to: (a) determine components of streamflow in catchments with different environmental conditions (Wang et al., 2008; Barras and Simmonds, 2008a,b; Vodila et al., 2011; Cai et al., 2015), (b) offer the evidence for precipitation end member of groundwater and surface water mixing and water balance (Holdsworth et al., 1991; You et al., 2014; Yu et al., 2016), (c) clarify the mechanisms controlling stream water behavior (Rozanski et al., 1993; Gammons et al., 2006; Ren et al., 2013; Zhai et al., 2013; Salamalikis et al., 2015), and (d) delineate flow paths and flow systems, and to model catchment residence times (Yang et al., 2011a,b; Li et al., 2014, 2016). It can be also treated as a tracer of moisture sources and rainout processes for regional air-masses to demarcate isotope-enabled regional or global circulation models and to study plant water uptake (Vodila et al., 2011; Ren et al., 2013; Zhai et al., 2013; Srivastava et al., 2014; You et al., 2015a, 2015b; Cai et al., 2015). In addition, it has been employed to investigate biogeochemical cycling and the mechanisms affecting stream water chemistry (Holdsworth et al., 1991; Li et al., 2015b; He and Richards, 2015).

δD and $\delta^{18}O$ are subject to fractionation (the δD and $\delta^{18}O$ value in water often decreases or increases in response to the changing of environmental factors, such as temperature, relative humidity) during phase changes, and their concentrations are sensitive to atmospheric parameters (Craig, 1961; Tian et al., 2007; Barras and Simmonds, 2008a,b). Both δD and $\delta^{18}O$ concentrations can be controlled by: (a) the isotopic composition of the water vapor sources, (b) the weather conditions at the vapor origin and the temperature at which condensation occurs, (c) the extend and trajectory of water vapor transportation (Rozanski et al., 1993; Gao et al., 2011; Vodila et al., 2011; Hughes and Crawford, 2013; Guo et al., 2014), and (d) the rainout history of the air mass and the precipitation amount (Araguás-Araguás et al., 2000; Argiriou and Lykoudis, 2006; Xie et al., 2011; Yu et al., 2013; Cui and Li, 2015).

In arid regions of China, the concentrations of $\delta^{18}O$ and δD of precipitation vary widely in time and space, and are controlled predominantly

* Corresponding author at: Cold and Arid Region Environment and Engineering Research Institute, Gansu Hydrology and Water Resources Engineering Research Center, CAS, Lanzhou 730000, China.
E-mail address: lizxhhs@163.com (L. Zongxing).

http://dx.doi.org/10.1016/j.atmosres.2016.07.023
0169-8095/

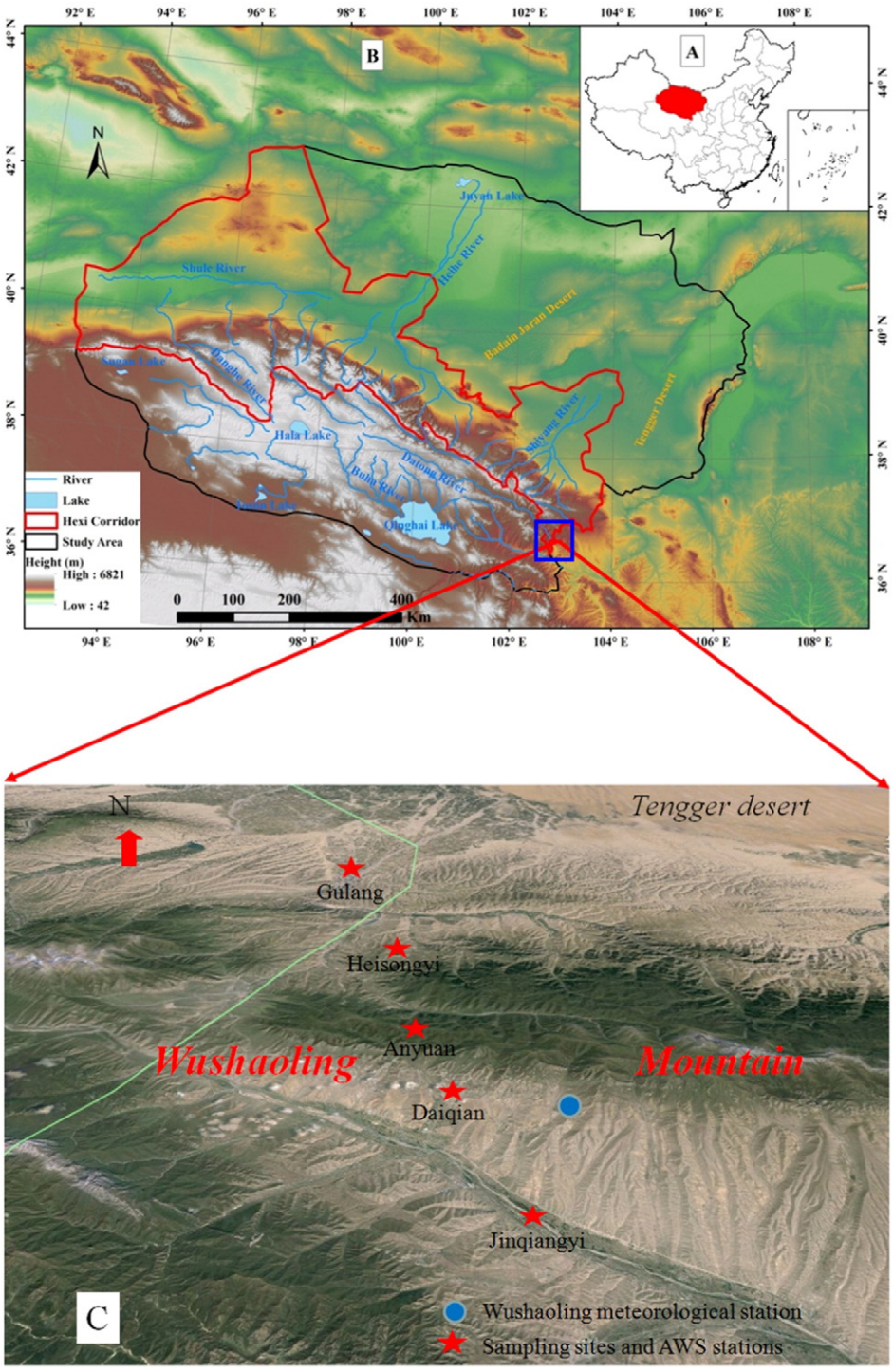

Fig. 1. Study region: A is the location for the Extensive Hexi Region, B is the location for Wushaoling Mountain, and C is five sampling stations.

Table 1
Sampling stations in Wushaoling Mountain.

Sampling sites	Location	Latitude	Longitude	Altitude(m)	Samples	Annual mean temperature(°C)	Annual precipitation(mm)	Relative humidity (%)	$\delta^{18}O$(‰)	δD(‰)	*d*-excess(‰)
Gulang	North slope	37.45°N	102.88°E	2085	66	9.5	398.5	58	−7.7	−46.	15.1
Heisongyi	North slope	37.35°N	102.9°E	2320	70	7.3	455.4	64	−7.8	−50.0	16.2
Anyuan	North slope	37.25°N	102.85°E	2700	115	4.9	535.6	74	−8.9	−54.9	17.9
Daiqian	South slope	37.22°N	102.57°E	3300	137	−0.7	642.3	81	−10.3	−66.7	18.0
Jinqiangyi	South slope	37.13°N	102.57°E	2800	80	4.3	354.1	75	−8.5	−52.5	15.2

by atmospheric properties (evaporation, temperature, and relative humidity etc.) and by geographic factors (altitude, latitude, moisture source, and transportation process etc.). Determining how the isotopic composition of modern precipitation is linked to today's climatic conditions provides a foundation for investigating past climate and environmental change (Aizen et al., 1996; Kreutz et al., 2003; Zhang and Wu, 2007; Wang et al., 2008; Wu et al., 2010; Zhao et al., 2011; Li et al., 2015a). In arid regions, precipitation is the most crucial part of the hydrological cycle. Its precipitation isotopic composition is an effective tracer for exploring the complex hydrologic processes and can be used to confirm the sources of water and system dynamics, the quantitatively estimate flow dynamics and transport parameters, the mean elevation of the recharge area of the aquifers, the length of hydrologic flow, and the transformation between surface water and groundwater (Kong and Pang, 2012; Li et al., 2015b,c,d; Sun et al., 2015; Zhou et al., 2015). Stable isotope studies in arid regions of China have also: (a) confirmed the Local Meteoric Water Line (LMWL) equation at regional and basin scales (Tian et al., 2001; Yang et al., 2011a,b; Ma et al., 2012); (b) described the temperature effect for the monthly and daily $\delta^{18}O$ variation (Pang et al., 2011; Kong et al., 2013; Guo et al., 2014); (c) observed the seasonal variation of $\delta^{18}O$ and *d*-excess (Li et al., 2015a; Fan et al., 2015; Wang et al., 2016); (d) discovered frequent exchange between groundwater and river water with the groundwater recharge and renewal in inland river basins (Zhang et al., 2009; Nie et al., 2010; Yang et al., 2011a,b); and (e) quantified the contribution from cryosphere meltwater to runoff in the inland river basins (Li et al., 2014, 2015b, 2015c, 2016).

However, there are no studies on the spatial and temporal variability of precipitation isotope composition related to the aspect of slopes in Qilian Mountains. Importantly, there is no clear understanding of the processes affecting the isotopic composition of precipitation in arid regions under the complex influences of variable atmospheric circulation, topography, sub-cloud evaporation, local environment factors and rainout process. Understanding of these processes is limited by the relatively sparse $\delta^{18}O$ and δD data in precipitation records in arid regions. In Wushaoling Mountain, previous research has identified rising temperatures and increases in precipitation (Jia et al., 2008; Qin et al., 2011), but there is no study has used stable isotopes to understand the processes influencing precipitation. In this study, $\delta^{18}O$ and δD concentrations are observed for 468 samples from individual precipitation events during the period July 2013 to June 2014 at three stations on the north slope and other two stations on the south slope of Wushaoling Mountain. The aims are as follows: (a) to explore the spatial and temporal variability of precipitation isotope composition and differences between the south and north slopes of Wushaoling Mountain; and (b) to confirm the effects of distant factors (moisture origin, rainout process) and local factors (temperature, altitude, sub-cloud evaporation) on isotopic variability. These results enhance knowledge of isotopic evolution in precipitation of arid regions and improve the understanding of the use of stable isotopes of precipitation for isotopic hydrology in inland river basins.

2. Data and methods

2.1. Study area

Wushaoling Mountain is located at the eastern end of the Qilian Mountains, on the northeastern edge of Tibetan Plateau in northwestern China (Fig. 1). The Qilian Mountains consist of several parallel mountains and valleys, stretching 850 km from northwest to southeast and extending 200–300 km from south to north. The altitude of about 30% of the mountains is above 4000 m, and its highest peak is Tuanjie Peak (height 5827 m). The air temperature varies with altitude, and the annual precipitation decreases from 700 mm on the south slope to 400 mm on the north slope. Qilian Mountains are very important to the Extensive Hexi Region because its precipitation and meltwater are important water sources for Shiyanghe, Heihe, and Shulehe rivers. Wushaoling Mountain (average elevation 3300 m a.s.l.) is considered as a crucial boundary between semi-arid and arid climate regions, and in-land and out-land river regions of China. The annual mean temperature and total

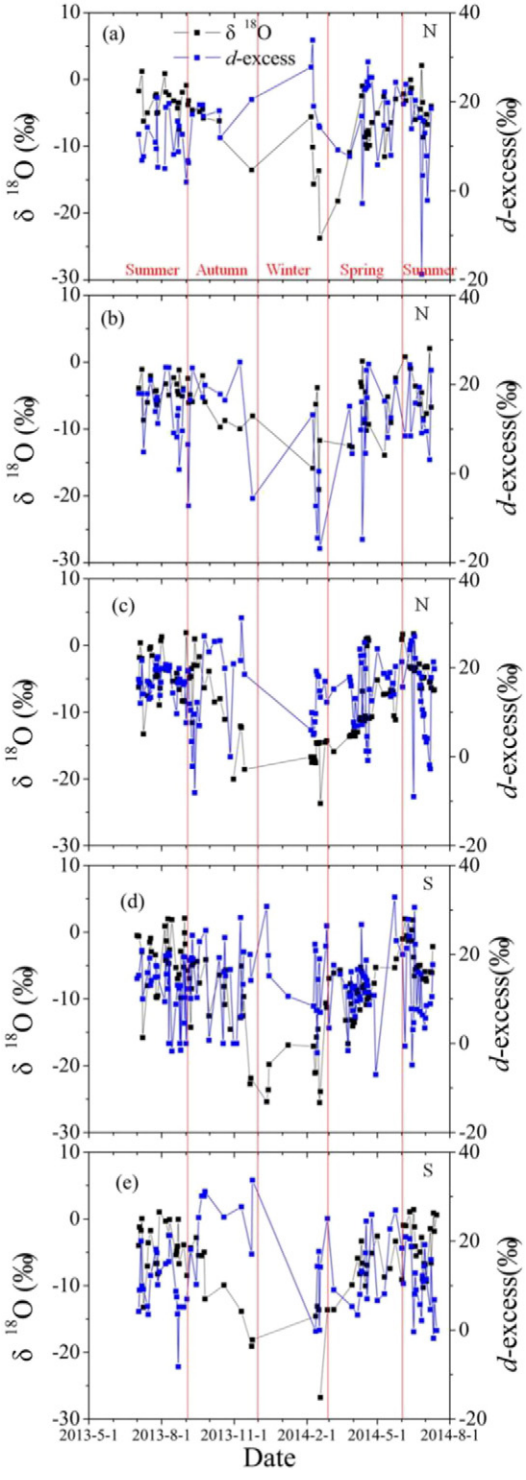

Fig. 2. The relationship between $\delta^{18}O$ and *d*-excess and its daily variation at Gulang (a),Heisongyi (b), Anyuan (c), Daiqian (d) and Jinqiangyi (e) ("N" and "S" in top right corner represents "North slope of Wushaoling" and "South slope of Wushaoling"; July–August of 2013 and June of 2014 is Summer, and September-November of 2013 is Autumn, and December of 2013 and January-February of 2014 is Winter, and March–May of 2014 is Spring).

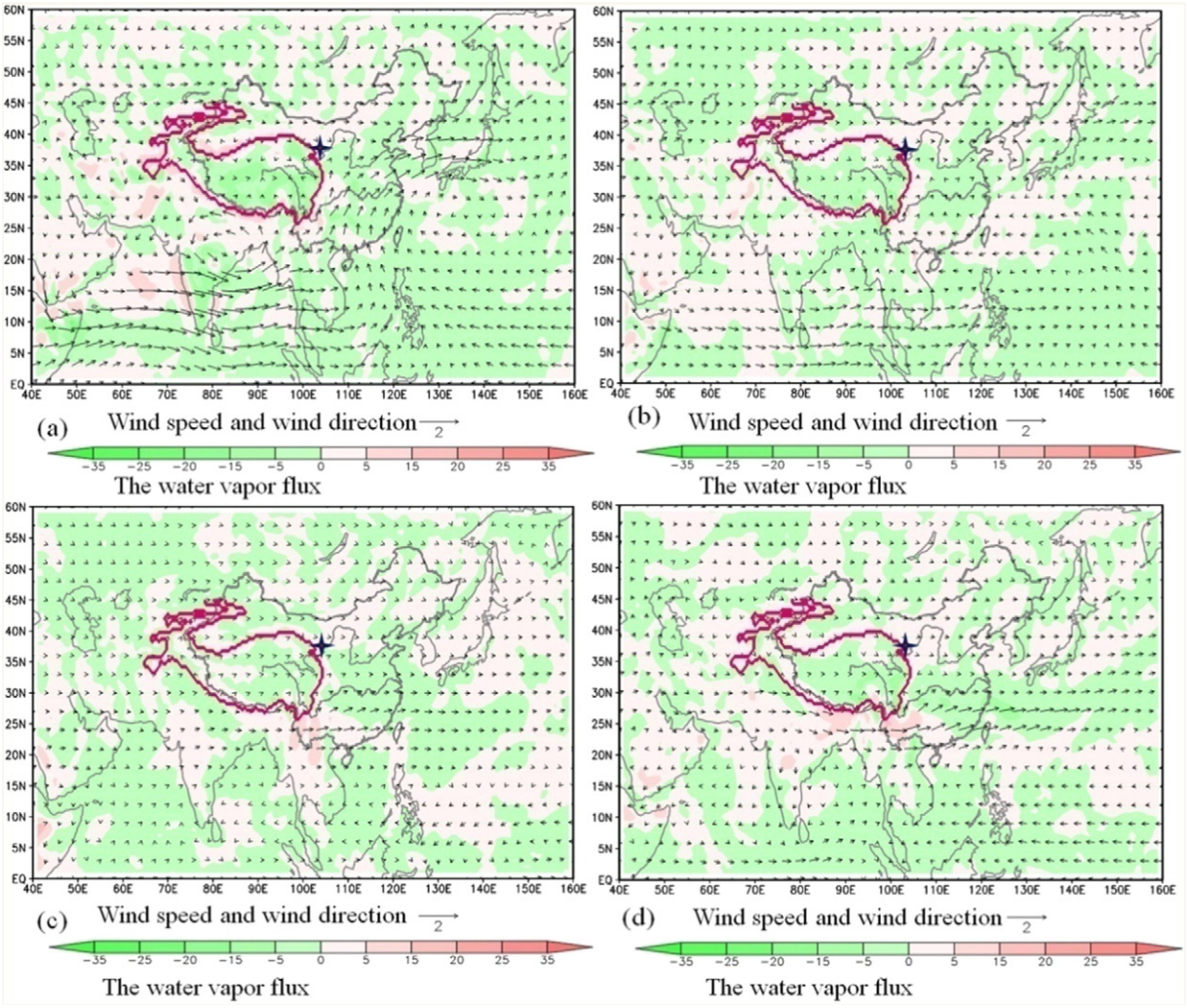

Fig. 3. Monthly water vapor transportation vectors at 700 hPa in July 2013 (a), September 2013 (b), February 2014 (c) and May 2014 (d) (the red tetragon is study region; the black arrow and number 2 are wind direction and wind speed; the red-green line is the water vapor flux).

precipitation are 0.13 °C and 400.8 mm, respectively, for the Wushaoling meteorological observation station (3023 m a.s.l., located at the Wushaoling pass between the north slope and south slope), and the temperature (0.27 °C/10a, significant at the 0.05 level) and precipitation (12.54 mm/10a, nonsignificant at the 0.05 level) have an increasing trend during the period of 1960–2014.

2.2. Samples and data

Precipitation samples were collected for precipitation events at five locations during from July 2013 to June 2014: Gulang, Heisongyi and Anyuan on the north slope, and Daiqian and Jinqiangyi on the south slope of Wushaoling Mountain (Fig. 1, Table 1). Each sample collector was placed on a rooftop (8 m above the ground and 1 m from the floor of the roof) away from the surface soil and any potential pollutant sources. Sampling was done manually on an event basis using a wet collector, which consisted of a 5-Lpolyethylene collecting flask (at the bottom) fitted with a polyethylene funnel 126 cm in diameter. The collected rainfall or snow was then loaded into pre-cleaned polyethylene sample bottles after each precipitation event. The collectors (flasks and funnels) were deployed at the onset of each precipitation event and were retrieved immediately after the flasks were filled or after the rainfall stopped. Prior to the installation of collectors, the funnels and flasks were carefully cleaned and dried (Al-Khashman, 2005a,b). In addition, stringent sampling protocols were followed at all times during sample collection and handling to assure samples were not contaminated at the 0.1 μeq/L level. Precautions were taken in both collection and analysis processes to avoid possible contamination of precipitation samples. A total of 468 event-based precipitation samples were collected in Wushaoling Mountain. During the sampling process, precipitation, temperature, wind speed and relative humidity were recorded at corresponding auto weather station (AWS). After collection, all samples were immediately sealed in plastic bags and stored in a cold laboratory at −18 °C. $\delta^{18}O$ and δD of precipitation were analyzed by means of laser absorption spectroscopy (liquid water isotope analyzer, Los Gatos Research DEL-100) at Key Laboratory of Ecohydrology of Inland River Basin, Chinese Academy of Sciences. Before analysis, they were stored in a refrigerator with the temperature set at −4 °C, so they could melt gradually without evaporation. Results are reported according to Vienna Standard Mean Ocean Water (VSMOW). Measurement precisions for $\delta^{18}O$ and δD were better than 0.5‰ and 0.2‰, respectively.

We used the HYSPLIT4 model (http://www.arl.noaa.gov/ready/hysplit4.html) resolution to investigate the pathways of the air masses arriving at the sampling sites. 10-day backward trajectories at a daily

temporal resolution were estimated to investigate the pathways of the air masses arriving at the sampling site (37.25°N, 102.57°E, 3300 m a.s.l.) at 12:00 Beijing time (04:00 UTC). Monthly mean geopotential height, wind fields, relative humidity, and air temperature at 700 hPa were from reanalysis R1 dataset, obtained from the National Oceanic and Atmospheric Administration-Cooperative Institute for Research in Environmental Sciences (NOAA-CIRES) Climate Diagnostics Center (available from http://www.esrl.noaa.gov/psd/data/gridded/data.ncep.reanalysis.html), which has been used in central Qilian Mountains (Li et al., 2015a). These data sets cover the period from January 1948 to the present with a spatial resolution of 2.5° × 2.5° and with continuous global coverage (Kalnay, 1996; Kistler et al., 2001). To quantify changes in large scale atmospheric circulation, monthly mean circulation composites during 2013–2014 were obtained. The water vapor flux has also been calculated on the basis of NCEP/NCAR reanalysis R1 dataset at 700 hPa (NCEP/NCAR Reanalysis 1), and the details of calculation methods were presented by Li et al. (2012a,b,c).

2.3. Evaluation on influence from sub-cloud evaporation on $\delta^{18}O$ composition

Sub-cloud evaporation increases the $\delta^{18}O$ of precipitation, whereas moisture recycling decreases the values of this parameter (Pang et al., 2011; Kong et al., 2013). Therefore, it is necessary to correct the measured $\delta^{18}O$ of precipitation under the effect of sub-cloud evaporation. Kong et al. (2013) and Froehlich et al. (2008) showed that the $\delta^{18}O$ of precipitation in the cloud base can be determined by:

$$\delta^{i}_{cloud\ \ base} = \left(1-\frac{\gamma^{i}}{\alpha^{i}}\right)\cdot\left(f^{\beta^{i}}-1\right) \tag{1}$$

Where $\delta^{i}_{cloud\ \ base}$ is the $\delta^{18}O$ of precipitation in the cloud base, i is '18 (^{18}O), and the equilibrium fraction factor for $\delta^{18}O$ is α, which can be dominated by the condensation temperature and can be calculated by:

$$10^{3}\ln\alpha^{18}O_{W-V} = 1.137\left(10^{6}/T^{2}\right)-0.4156\left(10^{3}/T\right)-2.0667 \tag{2}$$

Where T is the average temperature in the ground level. The β and γ are estimated by:

$$\beta^{i} = \frac{1-\alpha^{i}(D/D')^{n}(1-h)}{\alpha^{i}(D/D')^{n}(1-h)} \tag{3}$$

$$\gamma^{i} = \frac{\alpha^{i}h}{1-\alpha^{i}(D/D')^{n}(1-h)} \tag{4}$$

Where f is the remaining fraction of the raindrop mass, which depends on the initial radius (r_{in}), evaporation rate (v_{evap}) and fall time of the raindrop (t). The parameter h is the relative humidity, D′ and D are the diffusion constants of $^{1}H^{2}H^{16}O$ ($^{1}H^{1}H^{18}O$) and $^{1}H^{1}H^{16}O$ in air, and the

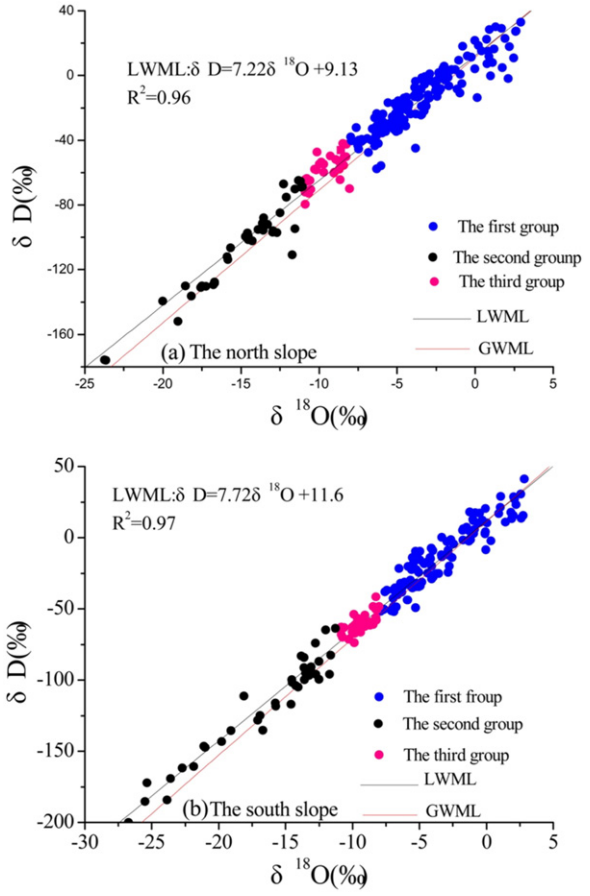

Fig. 4. Local meteoric water line (LMWL) for north slope (a) and south slope (b) of Wushaoling Mountain based on the data of individual sampling from July 2013 to June 2014 (the blue, black and red circles stand out three groups of stable isotope data).

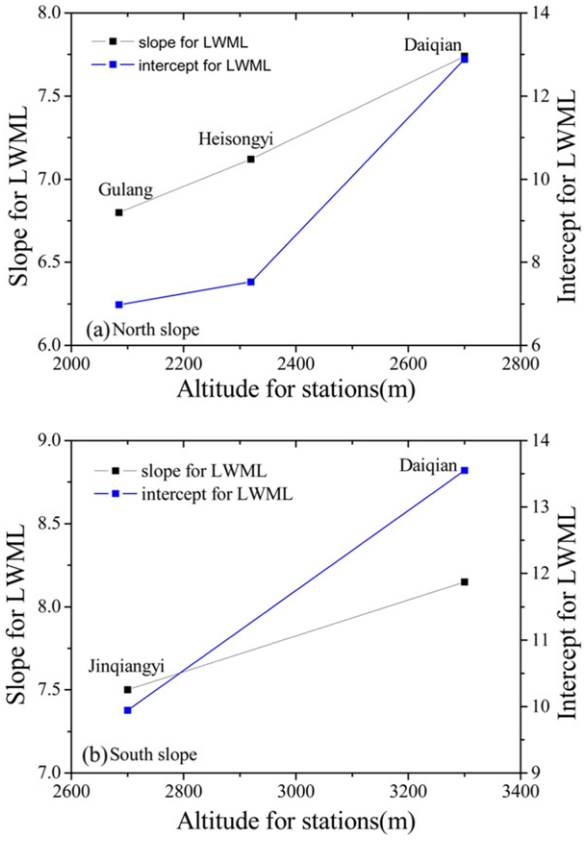

Fig. 5. Variation of slopes and intercepts of LWMLs with altitude on the north slope (a) and south slope (b).

ratio D/D′ is 1.024 (1.0289) (Stewart, 1975). The evaporation rate (f) of falling raindrops can be calculated by (Kinzer and Gunn, 1951):

$$f = 4\pi aD\left(1+\frac{Fa}{s'}\right)(\rho_a-\rho_b) \quad (5)$$

Where s′ represents the effective thickness of a shell around the raindrop, a is the radius of falling raindrops, ρ_a and ρ_b are density at the surface of the falling raindrop and in the ambient air, respectively, and F is a dimensionless quantity that measures the actual heat of moisture exchange. The part of eq. $D(\rho_a-\rho_b)$ is determined by humidity and temperature, and the part of Eq. (5) $(4\pi a(1+\frac{Fa}{s'}))$ is mainly determined by the raindrop size and ambient temperature. So the calculation of these two factors needs information on temperature, raindrop size and relative humidity (Kinzer and Gunn, 1951). The falling time of the raindrop can be estimated by falling velocity (v) and the distance between ground and cloud base. The falling velocity can be calculated using the following relationship (Best, 1950):

$$V = 9.58\left\{1-\exp\left[-\left(\frac{r}{0.885}\right)^{1.1471}\right]\right\} \quad (6)$$

Where r is the raindrop radius. The falling time is estimated by assuming that precipitation forms close to the average cloud base level (corresponding to the 850 hPa). Based on meteorological data, the effect of sub-cloud evaporation can then be determined.

The relative effect of sub-cloud evaporation on the composition of $\delta^{18}O$ can be defined as the sub-cloud evaporation enrichment rate of $\delta^{18}O$ (E), which can b estimated by:

$$F^i = \delta^i_{ground}-\delta^i_{cloud\ \ base} \quad (7)$$

$$E^i(\%) = 100\times\left(\frac{\delta^i_{ground}-\delta^i_{cloud\ \ base}}{\delta^i_{ground}}\right) = 100\times\left(-\frac{F^i}{\delta^i_{ground}}\right) \quad (8)$$

Where F^i is the difference between the isotopic composition of precipitation at the level of the ground sampling site and the cloud base respectively, and $\delta^i_{cloud\ \ base}$ is the composition of $\delta^{18}O$ for the cloud base precipitation, and δ^i_{ground} is the stable oxygen composition in precipitation at the ground sampling stations.

3. Results and discussions

3.1. Spatial and temporal pattern of stable isotopes

3.1.1. Temporal isotope variability

During the sampling period, the $\delta^{18}O$ values for precipitation varied from 4.0‰ to −26.8‰, with a mean value of −8.7‰. The δD values for precipitation varied from 17.0‰ to −199.9‰, with a mean value of −53.3‰. The *d*-excess fluctuated from −15.0‰ to 33.8‰ with a mean value of 16.5‰. In winter (from December to February of next year) $\delta^{18}O$, δD and *d*-excess values are-16.2‰, −116.6‰ and 16.6‰, respectively, while in summer (from June to August) they are −3.9‰, −18.1‰ and 8.9‰. Daily $\delta^{18}O$ values tend to decrease from July 2013 to February 2014 and then increase until June

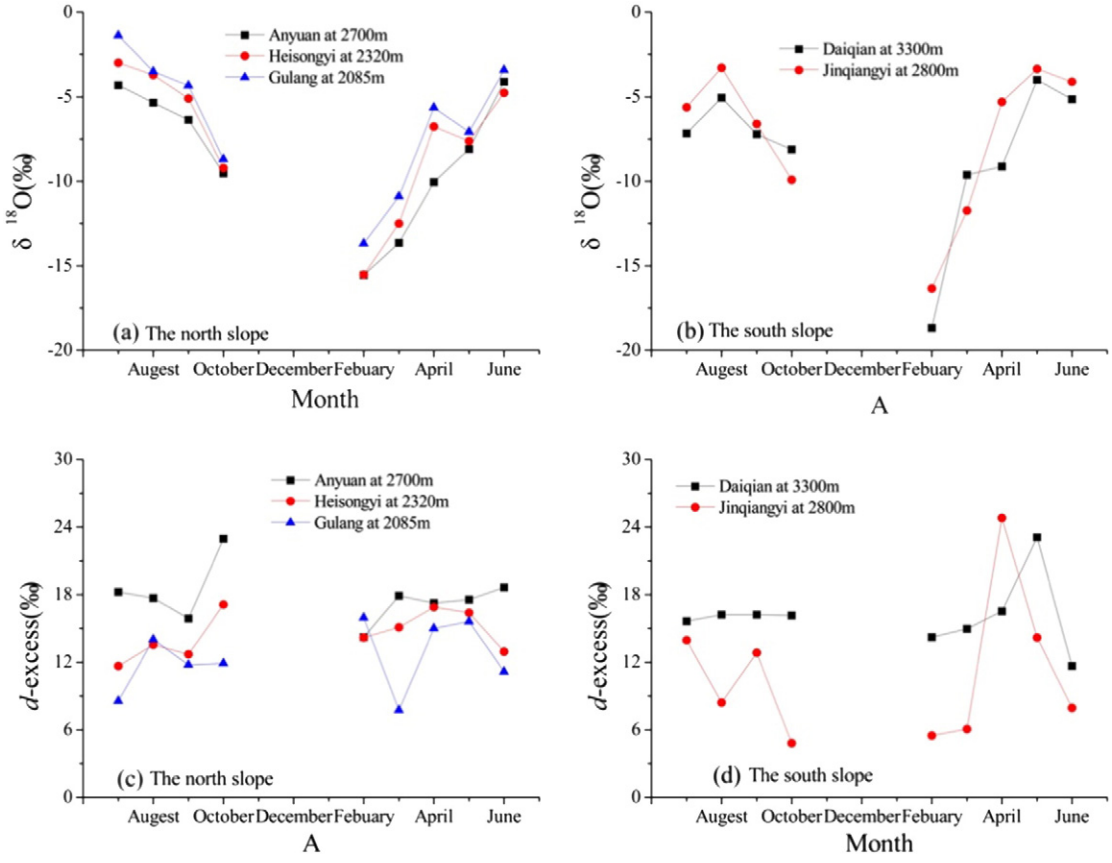

Fig. 6. Comparison for monthly $\delta^{18}O$ and *d*-excess in different altitudes on the north slope (a, b) and south slope (c, d).

2014 (Fig. 2). The lower values for $\delta^{18}O$ mainly occur in February, for example, the $\delta^{18}O$ is −23.7‰ on February 18, 2014 at Anyuan station and −25.5‰ on February 17, 2014 at Daiqian station. However, the $\delta^{18}O$ values for some precipitation events during summer can be low with high *d*-excess. These occurred on July 9, July 14 and August 27–30, 2013 on the north slope, and on July 9, July 14, July 25–27 and August 25, 2013 on the south slope. In addition, there are also some positive $\delta^{18}O$ values in summer; for example, the $\delta^{18}O$ is 2.0‰ on August 9, 2013 at Daiqian station, and it is 2.6‰ on August 6, 2013 at Anyuan station. *d*-excess tends to increase from July 2013 to February 2014 and then decrease until June 2014. Higher *d*-excess, values occur in winter and spring, while the lower values occur in summer and autumn. In general, the isotopic composition of precipitation is characterized by pronounced seasonal variation with higher $\delta^{18}O$ values in summer and lower $\delta^{18}O$ values in winter, while *d*-excess displays the opposite pattern (Fig. 2). The seasonal pattern observed for Wushaoling Mountain has also been observed in other arid regions of China, including the Wulumuqi river basin (Pang et al., 2011), Shiyanghe river basin (Ma et al., 2012) and Heihe river basin (Zhao et al., 2011).

The water vapor source of precipitation influences the temporal patterns of stable isotopes of precipitation in China (Tian et al., 2001, 2007; Guo et al., 2014; Li et al., 2015a; Yu et al., 2013). Fig. 3 shows the monthly water vapor transportation vector at 700 hPa for July 2013 (Fig. 3a), September 2013 (Fig. 3b), February 2014 (Fig. 3c) and May 2014 (Fig. 3d). Water vapor sources were primarily dominated by the westerly wind. However in July, the moisture from the Asia monsoon can arrive the North China including at Wushaoling Mountain. The relatively negative values of the stable isotopes, particularly in spring and winter, were due to the long distance transportation of water vapor. In addition, the influence of polar air masses, mainly in early spring (Tian et al., 2007; Zhao et al., 2011), is evident for some precipitation events with very low $\delta^{18}O$ and *d*-excess, such as on February 18, 2014 when the *d*-excess are 9.2‰, 6.8‰, 13.4‰, 7.0‰ and 9.1‰ for Gulang, Heisongyi, Anyuan, Daiqian and Jinqiangyi, respectively.

For some winter precipitation events, lower $\delta^{18}O$ are associated with higher *d*-excess values (e.g. November 21, 2013, December 15, 2013). These values can be associated with moisture originating from continental moisture recycling; or with rapid evaporation over relatively warm water bodies (e.g. Black, Caspian and Aral Seas) when the dry westerly air masses pass over them (Kreutz et al., 2003). These high *d*-excess values demonstrate that the local moisture recycling probably plays a very important role in local precipitation of Qilian Mountains (Zhou et al., 2007; Zhao et al., 2011; Li et al., 2015a). In general, high *d*-excess values are found in precipitation generated by evaporation of moisture under low relative humidity conditions and strong kinetic isotope fractionation. In contrast, the low *d*-excess values are derived from the evaporation of moisture under high relative humidity leading to the decrease of kinetic isotope fractionation (Dansgaard, 1964; Araguás-Araguás et al., 2000).

The relatively higher $\delta^{18}O$ and lower *d*-excess in summer and autumn are mainly caused by strong sub-cloud evaporation, which is created by raindrops falling from the cloud base to the ground. It is known that sub-cloud evaporation decreases the *d*-excess and increases the $\delta^{18}O$ of precipitation (Froehlich et al., 2008; Pang et al., 2011).

3.1.2. Spatial isotope variability

The equation of the Local Meteoric Water Line (LMWL) for Wushaoling Mountain, computed using all sampled data, is: $\delta D = 7.44\delta^{18}O + 9.32$, $R^2 = 0.96$ ($p < 0.01$; standard errors = 0.13). It has a lower slope and intercept than the Global Meteoric Water Line (GMWL), which indicates that a significant imbalance of isotope dynamic fractionation exists in arid climates. For both the north and south slopes, isotopic data can be classified into three groups with reference to the GMWL (Fig. 4). The first group comprises data points with high $\delta^{18}O$ values which are located at the top right corner of the figure, where some data points fall below the GMWL (*d*-excess < 10‰). These points correspond to precipitation events that occur mainly in summer and autumn when temperatures are higher. The second group comprises data points with low $\delta^{18}O$ values and are located in lower left, where points tend to fall above the GMWL (*d*-excess > 10‰). This second group mainly represents winter and spring precipitation occurring when both temperature and the absolute moisture content of air is

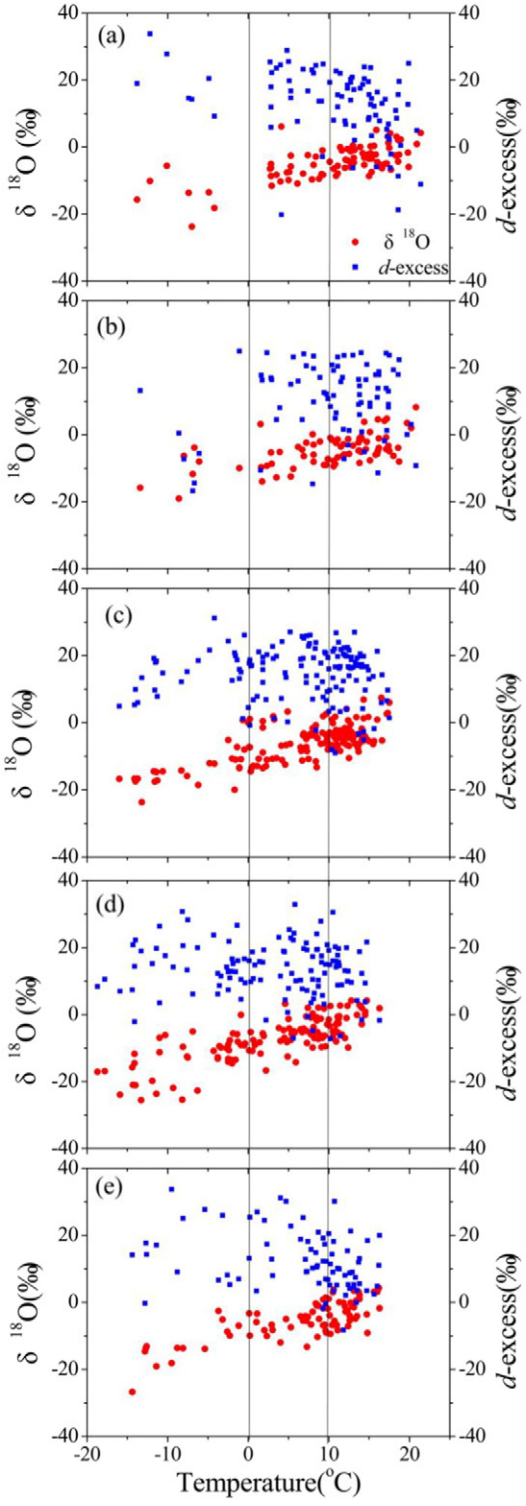

Fig. 7. Plot of temperature versus $\delta^{18}O$ and *d*-excess at Gulang (a), Heisongyi (b), Anyuan (c), Daiqian (d) and Jinqiangyi (e) in different temperature ranges (below 0 °C, from 0 to 10 °C, above 10 °C).

Table 2
Isotopic temperature effect for $\delta^{18}O$ and *d*-excess in different temperature ranges at five stations of Wushaoling Mountain[a].

Sampling sites	$\delta^{18}O$ gradient at temperature below 0 °C (‰°C^{-1}) (R^2)	$\delta^{18}O$ gradient at temperature 0–10 °C (‰°C^{-1}) (R^2)	$\delta^{18}O$ gradient at temperature above 10 °C (‰°C^{-1}) (R^2)	$\delta^{18}O$ gradient in all temperature range (‰°C^{-1}) (R^2)
Gulang	**0.63(0.15)**	0.16(0.01)	**0.58(0.27)**	**0.50(0.48)**
Heisongyi	**0.63(0.19)**	0.24(0.02)	**0.67(0.28)**	**0.47(0.24)**
Anyuan	**0.53(0.26)**	0.34(0.03)	**0.57(0.11)**	**0.34(0.48)**
Daiqian	**0.76(0.32)**	0.29(0.07)	**0.91(0.15)**	**0.58(0.50)**
Jinqiangyi	**1.05(0.62)**	0.09(0.06)	**0.85(0.19)**	**0.62(0.47)**
Sampling sites	*d-excess* gradient at temperature below 0 °C (‰°C − 1) (R^2)	*d-excess* gradient at temperature 0–10 °C (‰°C − 1)(R^2)	*d-excess* gradient at temperature above 10 °C (‰°C − 1) (R^2)	*d-excess* gradient at all temperature range (‰°C − 1) (R^2)
Gulang	**−1.48(0.4)**	0.04(0)	**−1.69(0.22)**	**−0.6(0.18)**
Heisongyi	**−3.6(0.77)**	−0.02(0)	**−1.19(0.09)**	**−0.43(0.15)**
Anyuan	**−0.57(0.2)**	−0.15(0.08)	**−0.7(0.1)**	**−0.3(0.09)**
Daiqian	**−0.17(0.1)**	−0.29(0.01)	−1.47(0.09)	**−0.23(0.12)**
Jinqiangyi	**−0.18(0.1)**	−0.17(0.03)	−0.74(0.09)	**−0.23(0.13)**

[a] Values for trends significant at the 5% level are set in bold.

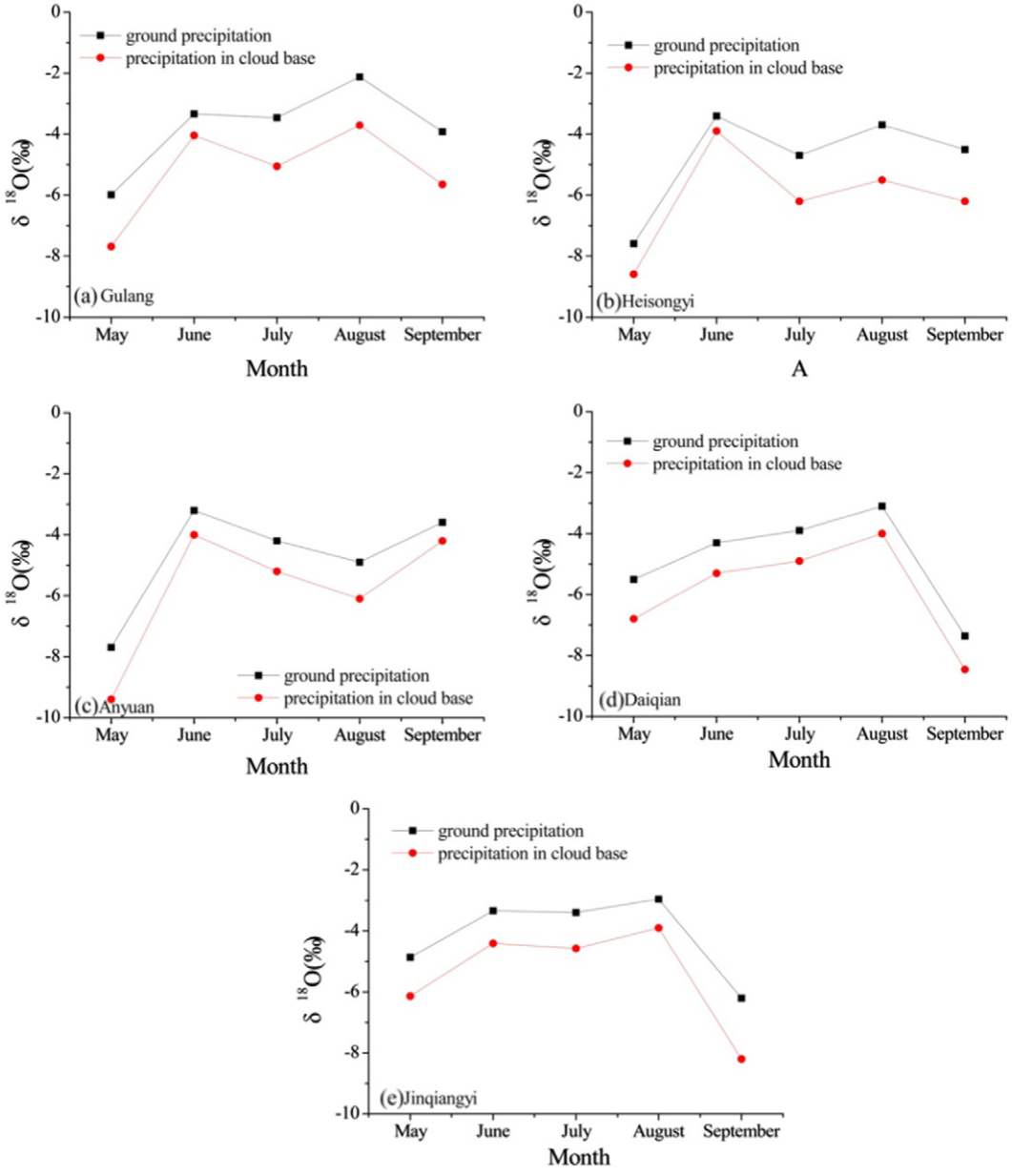

Fig. 8. Monthly average $\delta^{18}O$ of precipitation in the cloud base and ground in Gulang (a), Heisongyi (b), Anyuan (b), Daiqian (d) and Jinqiangyi (e).

Table 3
Isotopic composition of precipitation at the level of ground sampling site and the cloud base in the north and south slope of Wushaoling Mountain.

Location	$\delta^{18}O$ (‰)	May	June	July	August	September
North slope	Cloud base	−8.56‰	−3.98‰	−5.49‰	−5.1‰	−5.35‰
North slope	Ground	−7.1‰	−3.31‰	−4.12‰	−3.57‰	−4.01‰
South slope	Cloud base	−6.47‰	−4.85‰	−4.73‰	−3.95‰	−8.33‰
South slope	Ground	−5.18‰	−3.82‰	−3.64‰	−3.02‰	−2.84‰

low. The third group comprises data points with the intermediate $\delta^{18}O$ values that are closely aligned to the GMWL and are located between the first and second groups. The LMWL shows obvious differences between north and south slopes of Wushaoling Mountain (Fig. 4). The equation of LMWL is $\delta D = 7.22\delta^{18}O + 9.13$, $R^2 = 0.96$ ($p < 0.01$; standard errors = 0.16) on the north slope (Fig. 4a) and is $\delta D = 7.72\delta^{18}O + 11.60$, $R^2 = 0.97$ ($p < 0.01$; standard errors = 0.09) on the south slope (Fig. 4b). The slopes and intercepts of LMWL derived for each of the five stations are lower for sites on the north slope than for sites on the south slope, and also exhibit an increasing trend from lower to higher altitudes (Fig. 5).

Fig. 6 shows the monthly values for $\delta^{18}O$ decrease from Gulang to Anyuan station on the north slope and from Jinqiangyi to Daiqian station on the south slope, whereas *d*-excess increases with increasing altitude. The corresponding temperatures decreased by 4.6 °C and 5.0 °C during sampling periods, on the north and south slope, respectively. Owing to the different altitudes and local climate, there are noticeable differences of isotopic composition between the north slope and south slope. The average $\delta^{18}O$, δD and *d*-excess values are −8.1‰, −50.3‰ and 16.4‰, respectively, on the north slope, and −9.4‰, −59.6‰ and 16.6‰ on the south slope. This suggests there is a stronger imbalance of isotope dynamic fractionation on the north slope at lower altitudes. For

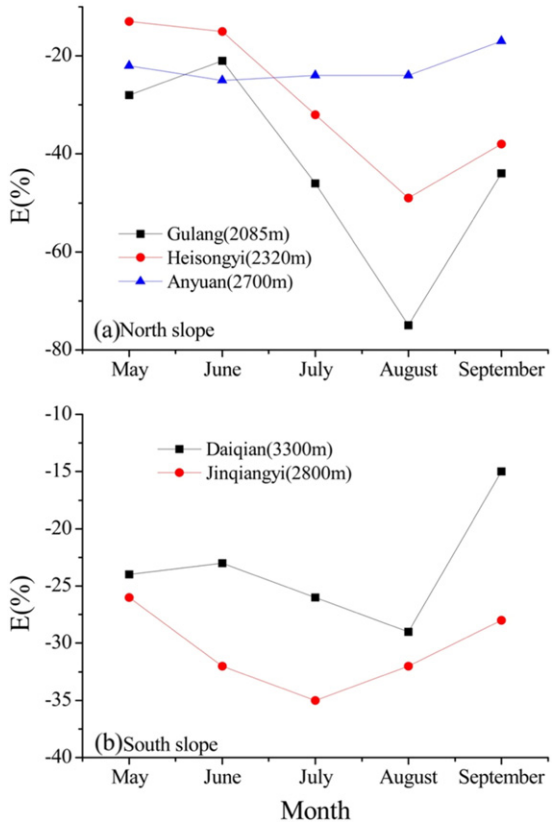

Fig. 9. Monthly variation of sub-cloud evaporation enrichment rate of $\delta^{18}O$ (E) on the north slope (a) and south slope (b).

d-excess, the higher altitude stations, Anyuan on the north slope and Daiqian on the south slope, have higher monthly average values than those values at lower altitudes, Gulang on the north slope and Jinqiangyi on the south slope (Fig. 6). This observation is consistent with previous studies that found values of *d*-excess in Qilian Mountains were higher than those in the plain of Hexi Corridor (Wang et al., 2008; Wu et al., 2010; Guo et al., 2014). This altitude effect of *d*-excess is similar to the one observed under more humid conditions where an increase of *d*-excess with the altitude was found (Froehlich et al., 2008). However, it is different from the Wulumuqi river catchments in eastern Tianshan Mountains, which are dominated by strong sub-cloud evaporation (Pang et al., 2011).

The pattern of *d*-excess variation is the opposite to the pattern of $\delta^{18}O$ in Wushaoling Mountain and therefore the two variables display negative correlation coefficients as follows: −0.19 for Daiqian at the altitude of 3300 m (not significant at the 0.05 level), and −0.31 for Jinqiangyi at the altitude of 2800 m (significant at the 0.05 level) on the south slope, respectively; −0.27 for Anyuan at the altitude of 2700 m (not significant at the 0.05 level), −0.46 and −0.59 for Heisongyi (2320 m) and Gulang (2085 m) on the north slope, and they are significant at the 0.05 level, respectively. The correlation coefficients display a decreasing trend from lower to higher altitudes, and there is no statistically negative correlation for Daiqian and Anyuan stations. This has also been observed at Hulugou station in the Middle Qilian Mountains (Li et al., 2015a) and the Altay station in China's northernmost mountainregion (Tian et al., 2007). However, a statistically significant negative correlation between *d*-excess and $\delta^{18}O$ for these GNIP stations with the relative lower altitudes in arid regions: Urumqi, Hetian, Zhangye, Lanzhou and Avalanche (Zhao et al., 2011; Li et al., 2012a,b,c). These facts reflect the different patterns of variation for $\delta^{18}O$ and *d*-excess between mountainous areas and plain areas in arid regions.

There could be two reasons for these differences in spatial variability: (1) The height of the cloud base (above the ground) and the saturation deficit are both higher for lower altitude stations, than for those at higher altitudes, and sub-cloud evaporation is assumed to be strengthened at low altitude stations. So sub-cloud evaporation dominated the isotopic evolution at lower altitude region under relatively high temperature, which would therefore increase $\delta^{18}O$ (tending to positive) and decrease *d*-excess (tending to negative) (Pang et al., 2011); (2) In higher altitudes stations, both the height of the cloud base and the saturation deficit are lower, and it is possible that sub-cloud evaporation is reduced in mountains sampling stations (Froehlich et al., 2008). Higher altitude precipitation is associated with low cloud temperature (Tian et al., 2007) and potentially weaker sub-cloud evaporation, such that moisture recycling dominates the evolution of isotopes in precipitation. Actual evapotranspiration is larger in the moist forest, meadow and grass present in the mountainous regions than in arid plain or foothill regions (Li et al., 2015a). Weaker sub-cloud evaporation and stronger evapotranspiration would decrease $\delta^{18}O$ (tending to negative) and increase *d*-excess (tending to positive). Many researchers have also concluded that moisture recycling is an important component of precipitation in the vast arid region of northwestern China (Pang et al., 2011; Zhao et al., 2011; Li et al., 2015a). Cui et al. (2009) confirmed the regional

Table 4
Isotopic precipitation amount effect in Wushaoling Mountain[a].

Sampling sites	Sampling period (‰ mm^{-1}) (R^2)	July of 2013 (‰ mm^{-1}) (R^2)	August of 2013 (‰ mm^{-1}) (R^2)	June of 2014 (‰ mm^{-1}) (R^2)
Gulang	−0.07(0.01)	−0.65(0.25)	0.06(0.05)	−0.14(0.13)
Heisongyi	−0.09(0.01)	−0.26(0.32)	−0.51(0.17)	−0.03(0.06)
Anyuan	0.21(0.03)	−0.12(0.01)	−0.15(0.05)	−0.09(0.05)
Daiqian	0.05(0.001)	−0.37(0)	−0.12(0.2)	−0.34(0.008)
Jinqiangyi	0.23(0.04)	−0.42(0.08)	−0.04(0.006)	−0.02(0)

[a] Values for trends significant at the 5% level are set in bold.

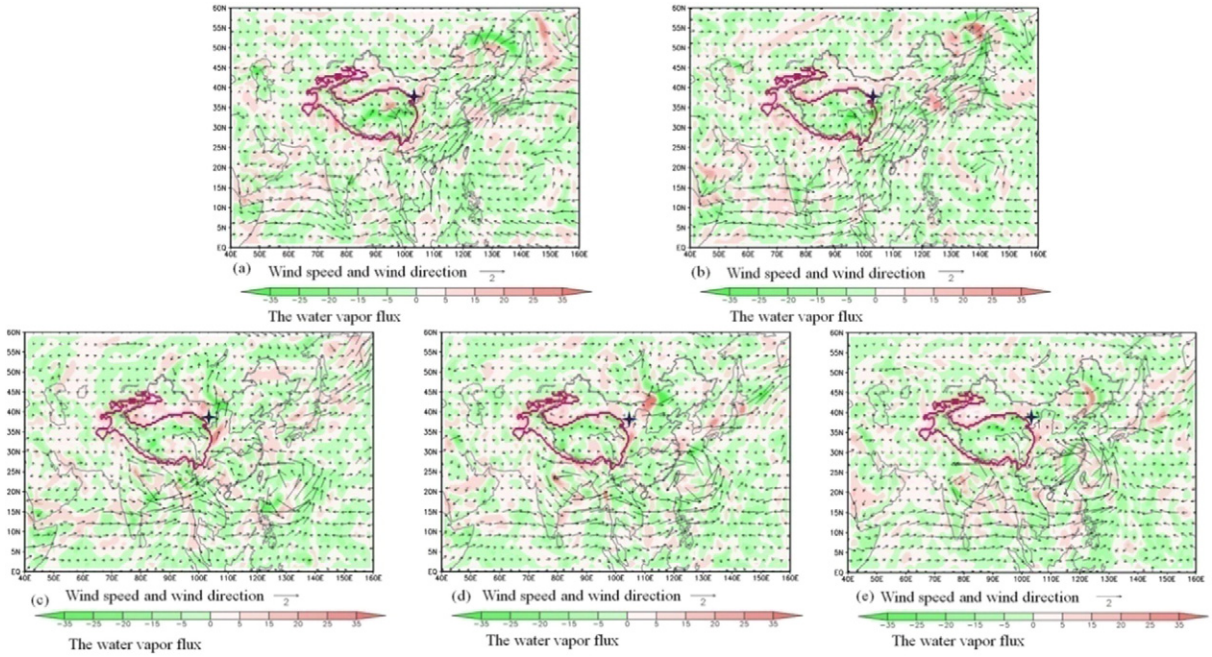

Fig. 10. Daily water vapor transportation vectors at 700 hPa for two typical monsoonal precipitation events: July 7 (a) and 8 (b), 2013; August 19 (c), 20 (d) and 21 (e), 2013 (the red tetragon is the study region; the black arrow and number 2 are wind direction and wind speed; the red-green line is the water vapor flux).

evapotranspiration moisture often generates precipitation at higher altitude regions, and suggested an eco-hydrological connection exists between the sub-alpine forests and the alpine meadow ecosystems, through secondarily evaporated precipitation.

3.2. Effects of local factors on stable isotopes

3.2.1. Temperature

Fig. 7 shows that the precipitation samples for all five stations can be divided into three groups based on temperature variation. The first group is related to temperatures above 10 °C with generally higher $\delta^{18}O$ and lower *d*-excess, and it appears that isotopic enrichment due to sub-cloud evaporation over-compensates for isotopic depletion by moisture recycling. This is supposed to be an indication of strong sub-cloud evaporation (Froehlich et al., 2008; Pang et al., 2011; Li et al., 2015a), and it can be confirmed by the statistically significant correlation between $\delta^{18}O$, *d*-excess and temperature for all five stations in Wushaoling Mountain (Table 2). These precipitation events mainly occur under high temperature and low relative humidity. Heavy sub-cloud evaporation can cause a decrease in *d*-excess and an increase in $\delta^{18}O$, which can be linked to a high vapor deficit and warm temperature when raindrops fall below the cloud base (Chen et al., 2007; Wu et al., 2010; Zhou et al., 2012; Ma et al., 2012). The second group is related to temperatures between 0 °C and 10 °C (Fig. 7). If the 'outliers' for these five stations are not included in this group, $\delta^{18}O$ and *d*-excess tends to be constant with temperature indicating moisture recycling. Froehlich et al. (2008) and Pang et al. (2011) suggested that stable isotope compositions decrease with increasing temperature. In this temperature range, an increase in moisture recycling appears to compensate for sub-cloud evaporation, which is clearly demonstrated by the non-significant correlation between stable isotopes and temperature (Table 2). The third group is related to low temperatures (temperature below 0 °C). It shows a clear temperature effect and linear relationship between $\delta^{18}O$, *d*-excess and temperature (Fig. 7), which can be also supported by the statistically significant correlation (Table 2). This suggests adiabatic cooling of rising air masses in mountainous terrain. Kinetic isotopic fractionation during snow formation is considered for the temperatures below 0 °C (Gat et al., 2001; Pang et al., 2011). The measured data and model simulations suggest that *d*-excess is only affected by such kinetic fractionation in winter.

As shown in Table 2, the $\delta^{18}O$-temperature coefficients for the third group (temperatures below 0 °C) are significantly higher than the second group (temperature from 0 °C to 10 °C) and when computed over all data at all five stations. This $\delta^{18}O$ (δD)-temperature relationship is consistent with the results derived from the Rayleigh model for equilibrium isotope fractionation, when precipitation events occur below 0 °C. These characteristics indicate that temperature effect fluctuates as a result of temperature variation. Rozanski et al. (1992) suggested that the isotope signature of precipitation over mid- and high-latitude regions is mainly controlled by regional-scale processes, especially the local temperature. In addition, the temperature effect is relatively larger on the south slope than that on the north slope (Table 2). Thus, temperature is a crucial determinant of precipitation isotope composition in study region and is associated with the process of equilibrium isotopic fractionation, sub-cloud evaporation and moisture recycling.

3.2.2. Altitude

The isotopic composition of precipitation becomes gradually depleted with clouds rising along the mountain slope (Gonfiantini et al., 2001). As shown in Table 1, the average $\delta^{18}O$ decreased with altitude, while *d*-excess increased. During the sampling period, the altitude gradients on the north slope for annual average, summer and winter $\delta^{18}O$ are −0.2‰/100 m ($p < 0.05$), −0.14‰/100 m ($p < 0.05$) and −0.28‰/100 m ($p < 0.05$). The corresponding values for δD are −1.2‰/100 m ($p < 0.05$), −0.52‰/100 m ($p < 0.05$) and −1.4‰/100 m ($p < 0.05$), respectively. On the south slope, the altitude gradients for annual average, summer and winter $\delta^{18}O$ are −0.32‰/100 m, −0.29‰/100 m and −0.38‰/100 m for $\delta^{18}O$; and −2.24‰/100 m, −1.54‰/100 m and −2.64‰/100 m for δD, respectively. This indicates that the altitude gradients changed with season, which is also supported by other studies in arid regions of China (Zhang and Wu, 2007; Wang et al., 2008; Wu et al., 2010; Pang et al., 2011; Guo et al., 2014; Li et al., 2015a). The altitude gradients on the south slope are relatively larger than those on the north slope. The reasons for this phenomenon are as follows: 1) the relative higher altitudes on the south slope with the dropping of temperature, which

usually leads to an enhanced moisture condensation in air mass and therefore to a progressive depletion in heavy isotopes of precipitation (Araguás-Araguás et al., 2000); 2) stronger sub-cloud evaporation leads to an increasing enrichment of $\delta^{18}O$ and δD in precipitation. Thus, it can cause a relatively lower altitude gradient in arid regions owing to the smaller $\delta^{18}O$ and δD gap between high altitude and low altitude. Taking the adiabatic cooling with altitude rise into account, this altitude gradient is also related to the temperature effect.

3.2.3. The influence from sub-cloud evaporation on $\delta^{18}O$ composition

Based on Kong et al. (2013), the average radius of water raindrop is 0.40 mm in Qilian Mountains and Hexi corridor. So using Eqs. (1)–(8), and the relevant meteorological parameter, the effect of sub-cloud evaporation on the $\delta^{18}O$ composition in precipitation was estimated for the months with temperatures above 0 °C (from May to September). Fig. 8 shows the $\delta^{18}O$ of precipitation in the cloud base is more negative than that of ground precipitation at five sampling stations, which reflects the enrichment of $\delta^{18}O$ under sub-cloud evaporation. The $\delta^{18}O$ values of precipitation in the cloud base is −8.56‰, −3.98‰, −5.49‰, −5.1‰ and −5.35‰ in May, June, July, August and September on the north slope, and the corresponding values in the ground precipitation is −7.1‰, −3.31‰, −4.12‰, −3.57‰ and −4.01‰ (Table 3), respectively. On the south slope, the $\delta^{18}O$ values of precipitation in the cloud base is −6.47‰, −4.85‰, −4.73‰, −3.95‰ and −8.33‰ in May, June, July, August and September, and the corresponding values in the ground precipitation is −5.18‰, −3.82‰, −3.64‰, −3.02‰ and −2.84‰ (Table 3), respectively. As a whole, the sub-cloud evaporation has enriched the $\delta^{18}O$ composition by 23%, 23%, 32%, 42% and 29% for May, June, July, August and September in the study region, and the corresponding values on the north slope are 21%, 20%, 34%, 49% and 33%, and on the south slope are 25%, 28%, 30%, 31% and 24%, respectively. This influence is stronger on the north slope than that on the south slope. Fig. 9 shows that the enrichment rate increased from May to a maximum in August and then decreased (Fig. 9). The sub-cloud evaporation enrichment rate of $\delta^{18}O$ (E) displayed a decreasing trend from lower altitude to higher altitude in study region (Fig. 9), which confirmed again the sub-cloud evaporation dominated the isotopic evolution in lower altitudes owing to the arid climate.

3.3. Effect of distant factors on stable isotopes

3.3.1. Monsoon moisture in synoptic scales

Monsoon precipitation can be characterized by isotope compositions showing a "precipitation amount effect" (the statistically negative correlation between precipitation amount and $\delta^{18}O$) in China (He et al., 2006; Pang et al., 2006; Tian et al., 2007; Yu et al., 2013). In Wushaoling Mountain, although there is no significant "precipitation amount effect" for all precipitation events at five stations, $\delta^{18}O$ showed some negative correlation with precipitation amount in July 2013 and June 2014, although the correlation coefficients are not significant at the 0.05 level (Table 4). This can be supported by some precipitation events with relatively negative $\delta^{18}O$ and higher precipitation amounts which occur concurrently on both the north slope and south slope. During July 7–8, the $\delta^{18}O$ decreased from −6.9‰ to −15.8‰, and the corresponding precipitation increased from 6.1 mm to 9.8 mm for Daiqian on the south slope. Concurrently, at Anyuan on the north slope, the $\delta^{18}O$ decreased from −7.2‰ to −13.3‰, and the corresponding precipitation increased from 7.2 mm to 8.8 mm. This was also observed during August 19–21, 2013. In Daiqian on the south slope, the $\delta^{18}O$ decreased from −5.3‰ to −8.3‰, and the corresponding precipitation increased from 8.8 mm to 12.4 mm, while in Anyuan on the north slope, the $\delta^{18}O$ decreased from −4.2‰ to −7.9‰, and the corresponding precipitation increased from 1.1 mm to 4.9 mm. As Fig. 10 showing, the daily water vapor transportation vector at 700 hPa for July 7–8 and August 19–21, 2013, confirm Asia monsoonal moisture arrived in the study region along the eastern margin of Tibetan Plateau. In addition, back trajectories of air masses also suggested that on July 8 and August 19, 2013 precipitation moisture was sourced from the monsoon circulation (Fig. 11). Therefore, it can be deduced that a weak negative correlation was displayed between precipitation and $\delta^{18}O$ at the synoptic scale owing to the influence from monsoonal moisture. Li et al. (2015a) have also verified the same phenomenon in the middle Qilian Mountains. Wu et al. (2010) suggested that there was no clear "precipitation amount effect" for monthly scale, but a slight "precipitation amount effect" has also been observed at synoptic scale in Heihe river basin. Yu et al. (2013) found that Asian summer monsoon can reach Lanzhou and Zhangye stations of northwestern China only during the most active periods, and these

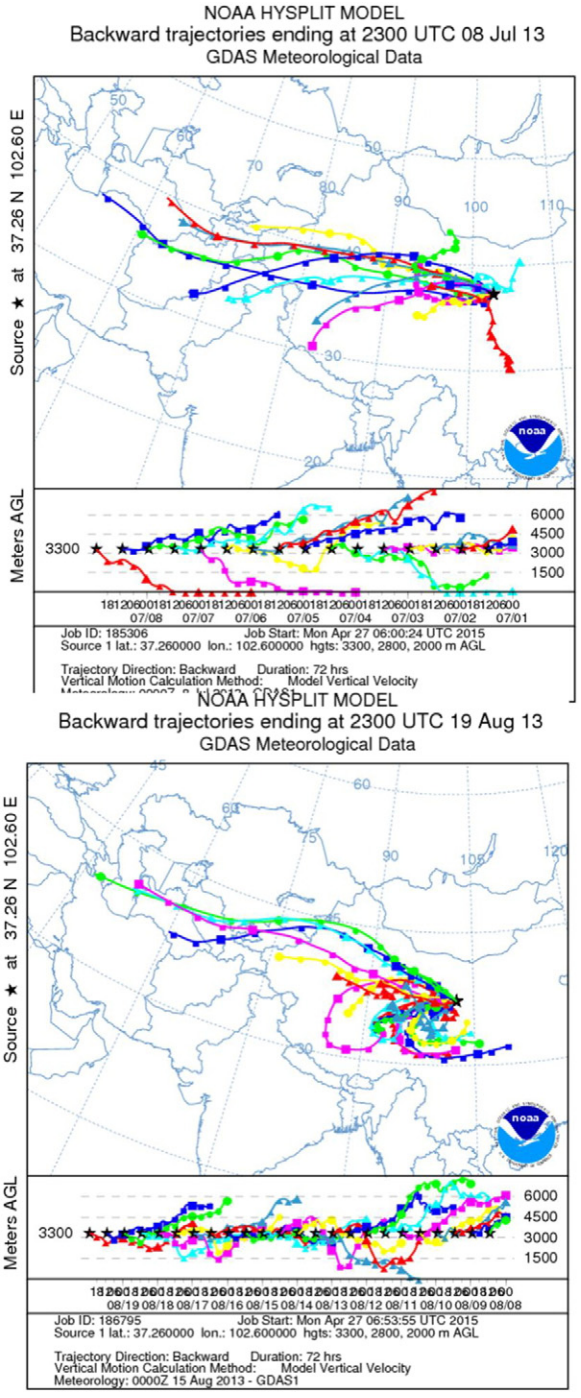

Fig. 11. Back trajectories for two monsoonal precipitation events: July 7 (a) and August 19 (b), 2013 (the black tetragon is study region).

summer precipitation events are with relatively depleted $\delta^{18}O$ values (<−7‰) and relatively higher temperatures (15 °C).

For the purpose of further investigating on the arrival of monsoon moisture, monthly composite circulation maps were created from NCEP/NCAR reanalysis data, covering the region of 0–70°N and 30–170°E. Wind vectors and geopotential heights at 700 hPa in July and August of 2013 are shown in Fig. 12. The largest differences (approximately 40 gpm) on the geopotential height composite are significant at 700 hPa. Two enhanced cyclonic circulations have developed, one is centered on Tibetan Plateau over China near 30°N and 90°E, and the other is centered near 55°N and 120°E. Meanwhile, a strong anticyclonic circulation has developed in the western Pacific near 25°N and 135°E. The enhanced low pressure pattern over the Eurasian continent suggests a strong East Asia summer monsoon. Under this atmospheric circulation, the southeasterly and southwesterly winds in China have been strengthened, which can arrive at Wushaoling Mountain along the eastern margin of Tibetan Plateau, and this can be also confirmed by the monthly water vapor transportation vector (Fig. 3d). These characteristics support the hypothesis that the Asian summer monsoon can reach Wushaoling Mountain during its most active periods in synoptic scales.

3.3.2. Rainout process

In addition to moisture sources, the rainout process also has some influence on the stable isotope composition of precipitation, as indicated by the daily variation of precipitation $\delta^{18}O$ for some continuous rainfall events (Fig. 13). As the duration of precipitation events increases, precipitation $\delta^{18}O$ can become more and more negative (Fig. 13). For example, precipitation $\delta^{18}O$ decreased from −2.8‰ to −8.5‰ over June 26–28, 2014 at Jinqiangyi station. This suggests that moisture was sourced from the same air mass during the period. Relatively positive $\delta^{18}O$ and δD were recorded even though there was a large amount of precipitation (3.5 mm) on June 26. However, there was relatively low precipitation (2.0 mm) and relatively negative $\delta^{18}O$ and δD on June 28. The temperature decreased from 12.1 °C on June 26 to 8.7 °C on June 27 and then increased to 9.4 °C on June 28, 2014. This phenomenon is common at all five stations for three multi-days precipitation events (Fig. 13). During these events the decreasing precipitation $\delta^{18}O$ is not related to temperature or precipitation amount. Thus, this phenomenon can be explained on the basis of leaching and Rayleigh distillation effects during precipitation, which deplete the composition of $\delta^{18}O$ and δD in water (Clark and Fritz, 1997). At the beginning of precipitation events, water vapor was enriched in $\delta^{18}O$ and δD when generating precipitation. But as precipitation event

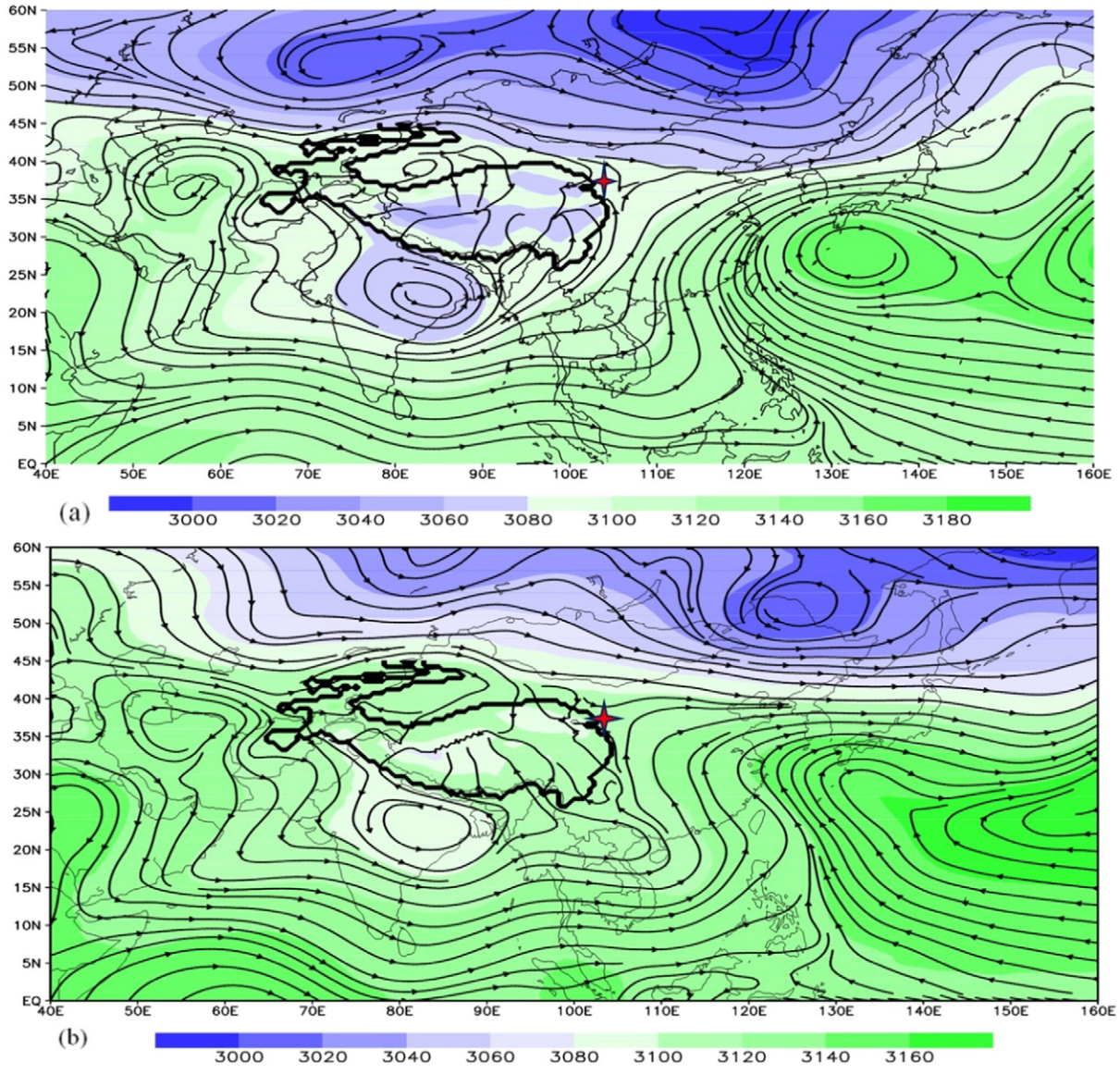

Fig. 12. Wind vectors and geopotential height for July (a) and August (b) of 2013 at 700 hPa.

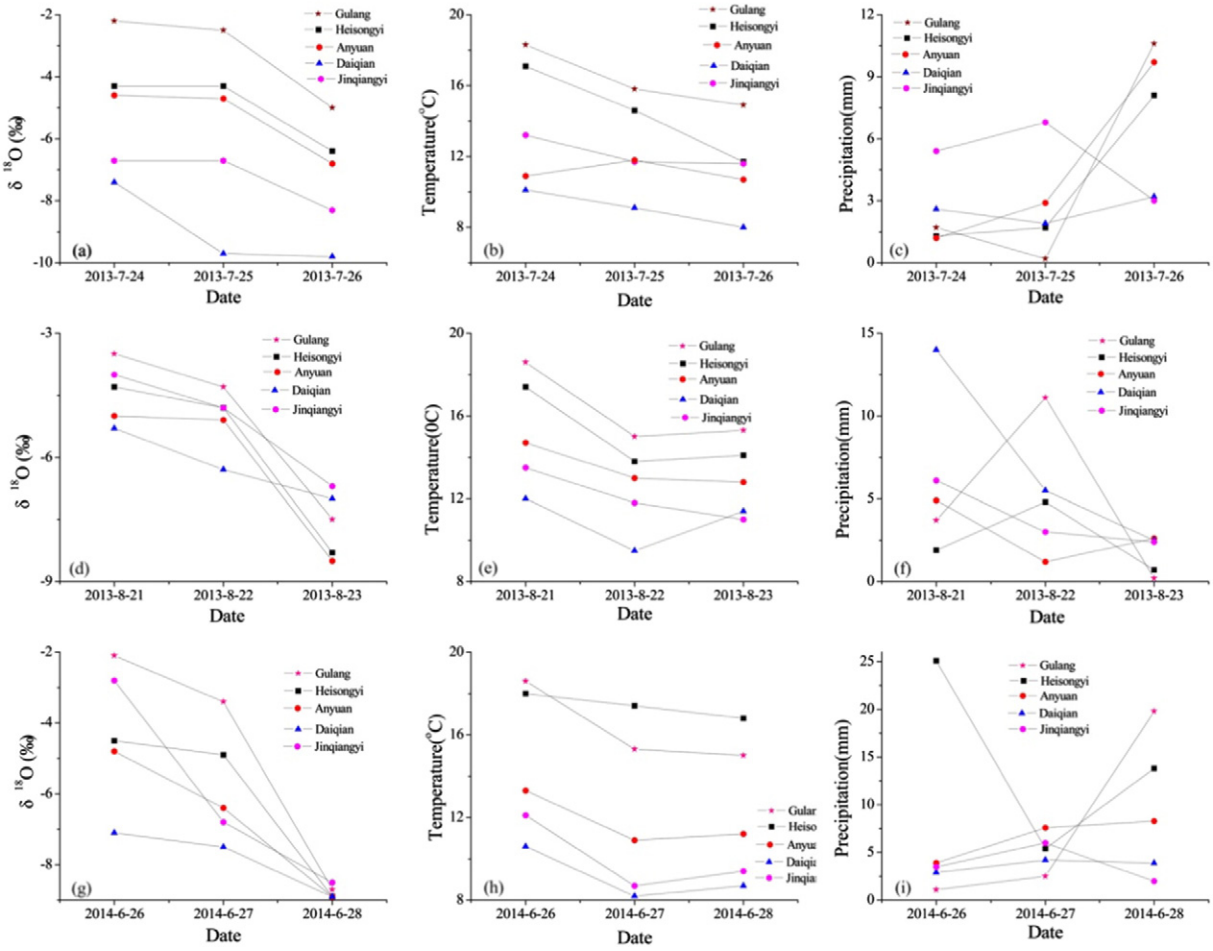

Fig. 13. Daily variation of $\delta^{18}O$ composition, temperature and precipitation for three continuous rainfall events in Wushaoling Mountain.

continued, it is progressively depleted for $\delta^{18}O$ and δD due to the influence of the rainout process.

4. Conclusion

The spatial-temporal characteristics of precipitation isotope compositions showed some differences between the southern and north slopes of Wushaoling Mountain. The average values of $\delta^{18}O$, δD and *d*-excess are −8.1‰, −50.3‰ and 16.4‰ on the north slope, and −9.4‰, −59.6‰ and 16.6‰ on the south slope, respectively. $\delta^{18}O$ decreased with increasing altitude, while *d*-excess increased. The slopes and intercepts of LWMLs on the north slope are lower than those on the south slope, and they generically increase with altitude. Although seasonal variation of $\delta^{18}O$ and *d*-excess showed similar patterns on both the north and south slopes, the correlation coefficients between $\delta^{18}O$ and *d*-excess displayed a decreasing trend from lower to higher altitudes, and there is no statistically negative correlation for Daiqian and Anyuan stations owing to weakening sub-cloud evaporation. Altitude gradients changed with season, and they are −0.2‰/100 m, −0.14‰/100 m and −0.28‰/100 m on the north slope for annual average, summer and winter $\delta^{18}O$, while the values on the south slope are −0.32‰/100 m, −0.29‰/100 m and −0.38‰/100 m, respectively.

In Wushaoling Mountain, temperature is a crucial factor for further isotopic evolution because it is associated with equilibrium fractionation and sub-cloud evaporation. Sub-cloud evaporation enriched $\delta^{18}O$ composition in May, June, July, August and September for the whole study region by 23%, 23%, 32%, 42% and 29%. $\delta^{18}O$ enrichment on the north slope was 21%, 20%, 34%, 49% and 33% for May, June, July, August and September, and 25%, 28%, 30%, 31% and 24%, respectively, on the south slope. Sub-cloud evaporation dominated isotopic evolution at low altitudes resulting in increased $\delta^{18}O$ and decreased *d*-excess. Moisture recycling was most influential on the isotopic evolution at higher altitudes due to stronger evaporation of the moist forest, meadow and grass present in the mountainous region than at arid plain or foothill region. Westerly winds principally dominate Wushaoling Mountain, so the relatively negative stable isotope values observed are related to the long distance transportation of water vapor in spring and winter. The relatively higher $\delta^{18}O$ and the lower *d*-excess in summer and autumn are mainly attributed to locally strong sub-cloud evaporation. In some circumstances, $\delta^{18}O$ and δD were depleted at the end of rainfall event due to the rainout process. In addition, some negative $\delta^{18}O$ in summer caused by monsoonal moisture which can arrive Wushaoling Mountain when an enhanced cyclonic circulation has developed on Tibetan Plateau and a strong anti-cyclonic circulation has developed in the western Pacific. Thus, strengthened southeasterly and southwesterly winds can reach Wushaoling Mountain along the eastern margin of Tibetan Plateau. The study enhances the knowledge of isotopic evolution in precipitation, and provides a basis for further study of isotopic hydrology study in arid regions.

Acknowledgments

This study was supported by a West Light Program for Talent Cultivation of Chinese Academy of Sciences (2013128), Gansu Province Science Fund for Distinguished Young Scholars (1506RJDA282), National Natural Science Foundation (91547102), by the CAS/SAFEA International Partnership Program for Creative Research Teams, A postdoctoral fellow at the international exchange plans from China Postdoctoral

Association (20140043), and by the Youth Innovation Promotion Association, CAS (2013274). We greatly appreciate suggestions from three anonymous referees for the improvement of our paper. Thanks to David Robertson for enhancement of English writing. Thanks also to the editorial staff.

References

Aizen, V., Aizen, E., Melack, J., Martma, T., 1996. Isotopic measurements of precipitation on central Asian glaciers (southeastern Tibet, north Himalayas, central Tien Shan). J. Geophys. Res 101 (D4), 9185–9196.

Al-Khashman, O.A., 2005a. Ionic composition of wet precipitation in the Petra region, Jordan. Atmos. Res 78, 1–12.

Al-Khashman, O.A., 2005b. Study of chemical composition in wet atmospheric precipitation in Eshidiya area, Jordan. Atmos. Environ 39, 6175–6183.

Araguás-Araguás, L., Froehlich, K., Rozanski, K., 2000. Deuterium and oxygen-18 isotope composition of precipitation and atmospheric moisture. Hydrol. Process 14, 1341–1355.

Argiriou, A.A., Lykoudis, S., 2006. Isotopic composition of precipitation in Greece. J. Hydrol 327, 486–495.

Barras, V.J.I., Simmonds, I., 2008a. Synoptic controls upon $\delta^{18}O$ in south Tasmanian episodic events. J. Geophys. Res 102 (C12), 2681–2687.

Barras, V.J.I., Simmonds, I., 2008b. Synoptic controls upon $\delta^{18}O$ in south Tasmanian precipitation. Geophys. Res. Lett 35, L02707.

Best, A.C., 1950. Empirical formulae for the terminal velocity of water drops falling through the atmosphere. Q. J. R. Meteorol. Soc. 76, 302–311.

Cai, M.Y., Wang, L.X., Parkes, S.D., Strauss, J., McCabe, M.F., Evans, J.P., Griffiths, A.D., 2015. Stable water isotope and surface heat flux simulation using ISOLSM: evaluation against in-situ measurements. J. Hydrol 523, 67–78.

Chen, S.Y., Dong, A.X., Han, T., 2007. Differences in summer precipitation between the east and west of the Qilian Mountains and its contributing factors. J. Nanjing Inst. Meteorol 30 (5), 715–719 In Chinese.

Clark, I., Fritz, P., 1997. Environmental Isotopes in Hydrogeology. Lewis Publishers, New York.

Craig, H., 1961. Isotopic variations in meteoric waters. Science 133, 1702–1703.

Cui, B.L., Li, X.Y., 2015. Runoff processes in the Qinghai Lake Basin, Northeast Qinghai-Tibet Plateau, China: insights from stable isotope and hydrochemistry. Quat. Int. 383, 1–10.

Cui, J., An, S.Q., Wang, Z.S., Fang, C.M., Liu, Y.H., Yang, H.B., Xu, Z., Liu, S.R., 2009. Using D-excess to determine the sources of high-altitude precipitation: implications in hydrological relations between sub-alpine forests and alpine meadows. J. Hydrol 373 (2009), 24–33.

Dansgaard, W., 1964. Stable isotopes in precipitation. Tellus 16, 436–468.

Fan, Y.T., Chen, Y.N., Li, X.G., Li, W.H., Li, Q.H., 2015. Characteristics of water isotopes and ice-snowmelt quantification in the Tizinafu River, north Kunlun Mountains, Central Asia. Quat. Int. 380-381, 116–122.

Froehlich, K., Kralik, M., Papesch, W., Rank, D., Scheifinger, H., et al., 2008. D-excess in precipitation of alpine regions-moisture recycling. Isot. Environ. Health Stud 44 (1), 61–70.

Gammons, C.H., Poulson, S.R., Pellicori, D.A., Reed, P.J., Roesler, A.J., Petrescu, E.M., 2006. The hydrogen and oxygen isotopic composition of precipitation, evaporated mine water, and river water in Montana, USA. J. Hydrol 328, 319–330.

Gao, J., Masson-Delmotte, V., Yao, T., Tian, L.D., Risi, C., Hoffmann, G., 2011. Precipitation water stable isotopes in the South Tibetan Plateau: observations and modeling. J. Clim 24, 3161–3178.

Gat, J.R., Mook, W.G., Meijer, H.A.J., 2001. Stable isotopes processes in the water cycle. In: Mook, W.G. (Ed.), Environmental Isotopes in the Hydrological Cycle (Principles and Applications), Atmospheric Water. UNESCO and IAEA, Paris, pp. 17–40.

Gonfiantini, R., Roche, M.A., Olivry, J.C., Fontes, J.C., Zuppi, G.M., 2001. The altitude effect on isotopic composition of tropical rains. Chem. Geol 181, 147–167.

Guo, X.Y., Feng, Q., Wei, Y.P., Li, Z.X., Liu, W., 2014. An overview of precipitation isotopes over the extensive Hexi region in NW China. Arab. J. Geosci http://dx.doi.org/10.1007/s12517-014-1521-9.

He, S.Y., Richards, K., 2015. The role of dew in the monsoon season assessed via stable isotopes in an alpine meadow in Northern Tibet. Atmos. Res 152, 101–109.

He, Y.Q., Pang, H.X., Theakstone, W.H., Zhang, Z.L., Lu, A.G., Gu, J., 2006. Isotopic variations in precipitation at Bangkok and their climatological significance. Hydrolo. PRO 20 (13), 2873–2884.

Holdsworth, G., Fogarasi, S., Krouse, H., 1991. Variation of the stable isotopes of water with altitude in the Saint Elias Mountains of Canada. J. Geophys. Res 96, 7483–7494.

Hughes, C.E., Crawford, J., 2013. Spatial and temporal variation in precipitation isotopes in the Sydney Basin, Australia. J. Hydrol 489, 42–55.

Jia, W.X., He, Y.Q., Li, Z.X., Pang, H.X., Yuan, L.L., Ning, B.Y., Song, B., Zhang, N.N., 2008. The regional difference and catastrophe of climatic change in Qilian Mt. Region. Acta Geograph. Sin 63 (3), 257–269 In Chinese.

Kalnay, E., 1996. The NCEP/NCAR 40-year reanalysis project. Bull. Am. Meteorol. Soc. 77, 437–471.

Kinzer, G.D., Gunn, R., 1951. The evaporation, temperature and thermal relaxation-time of freely falling water drops. J. Meteorol 8, 71–83.

Kistler, R., Kalnay, E., Collins, W., Saha, S., White, G., Woollen, J., Challiah, M., Ebisuzaki, W., Kanamitsu, M., Kousky, V., VandenDool, H., Jenne, R., Fiorino, M., 2001. The NCEP-NCAR 50-year reanalysis: monthly means CD-ROM and documentation. Bull. Am. Meteorol. Soc. 82, 247–267.

Kong, Y.L., Pang, Z.H., 2012. Evaluating the sensitivity of glacier rivers to climate change based on hydrograph separation of discharge. J. Hydrol 434-435, 121–129.

Kong, Y.L., Pang, Z.H., Froehlich, K., 2013. Quantifying recycled moisture fraction in precipitation of an arid region using D-excess. Tellus B 65, 19251. http://dx.doi.org/10.3402/tellusb.v65i0.19251.

Kreutz, K.J., Wake, C.P., Aizen, V.B., Cecil, L.D., Synal, H.A., 2003. Seasonal deuterium excess in a Tien Shan ice core: influence of moisture transport and recycling in Central Asia. Geophys. Res. Lett 30 (18), 1922. http://dx.doi.org/10.1029/2003GL017896.

Li, Z., He, Y., Wang, P., Theakstone, W.H., An, W., Wang, X., Lu, A., Zhang, W., Cao, W., 2012a. Changes of daily climate extremes in southwestern China during 1961–2008. Glob. Planet. Chang 80-81, 255–272.

Li, L.P., Li, Y.J., Liu, M.C., 2012b. Change trend of pan evaporation and its causes in Shiyang river basin during 1962–2005. J. Des. Res 32 (3), 832–841 In Chinese.

Li, X.F., Zhang, M.J., Li, Y.J., Wang, S.J., H, X.Y., Ma, Q., Ma, X.N., 2012c. Characteristics of $\delta^{18}O$ in precipitation and moisture transports over the arid region in Northwest China. Environ. Sci 33 (3), 710–719 In Chinese.

Li, Z.X., Feng, Q., Liu, W., Wang, T.T., Chen, A.F., Gao, Y., Guo, X.Y., Pan, Y.H., Li, J.G., Guo, R., Jia, B., 2014. Study on the contribution from cryosphere to runoff in the cold alpine basin: a case study of Hulugou River basin in the Qilian Mountains. Glob. Planet. Chang 122 (2014), 345–361.

Li, Z.X., Gao, Y., Wang, Y.M., Pan, Y.H., Li, J.G., Chen, A.F., Wang, T.T., Han, C.T., Song, Y.X., Theakstone, W.H., 2015a. Can monsoon moisture arrive Qilian Mountains in summer? Quat. Int. 358 (2015), 113–125.

Li, Z.X., Feng, Q., Liu, W., Wang, T.T., Guo, X.Y., Li, Z.J., Gao, Y., Pan, Y.H., Guo, R., Jia, B., Song, Y.X., Han, C.T., 2015b. The stable isotope evolution in Shiyi glacier system during the ablation period in the north of Tibetan Plateau, China. Quat. Int. 380-381, 262–271.

Li, Z.X., Feng, Q., Li, J.G., Pan, Y.H., Wang, T.T., Liu, L., Guo, X.Y., Gao, Y., Guo, R., Jia, B., 2015c. Environmental significance and hydrochemical processes at a cold alpine basin in the Qilian Mountains. Environ. Earth Sci 73 (8), 4043–4052.

Li, Z.X., Feng, Q., Guo, X.Y., Gao, Y., Pan, Y.H., Wang, T.T., Li, J.G., Guo, R., Jia, B., Song, Y.X., Han, C.T., 2015d. The evolution and environmental significance of glaciochemistry during the ablation period in the north of Tibetan Plateau, China. Quat. Int. 374, 93–109.

Li, Z.X., Feng, Q., Wang, Q.J., Song, Y., Cheng, A.F., Li, J.G., 2016. Contribution from frozen soil meltwater to runoff in an in-land river basin under water scarcity by isotopic tracing in northwestern China. Glob. Planet. Chang 136 (2016), 41–51.

Ma, J.Z., Zhang, P., Zhu, G.F., 2012. The composition and distribution of chemicals and isotopes in precipitation in the Shiyang River system, northwestern China. J. Hydrol 436-437, 92–101.

Nie, Z.L., Chen, Z.Y., Zhang, G.H., 2010. Groundwater recharge and renewal in the Minle Piedmont plain of the Heihe River basin. Hydrogeol. Eng. Geol 37 (2), 6–9 In Chinese.

Pang, H.X., He, Y.Q., Lu, A.G., Zhao, J.D., Ning, B.Y., Yuan, L.L., Song, B., 2006. Synoptic-scale variation of $\delta^{18}O$ in summer monsoon rainfall at Lijiang, China. Chin. Sci. Bull 51 (23), 2897–2904.

Pang, Z., Kong, Y., Froehlich, K., Huang, T., Yuan, L., 2011. Processes affecting isotopes in precipitation of an arid region. Tellus 63B, 352–359.

Qin, J., Ding, Y.J., Ye, B.S., Wang, Y., 2011. Influence of two patterns of El Nino on hydrological and meteological elements in Hexi corridor region of China. Plateau Meteorol 30 (5), 1279–1285 In Chinese.

Ren, W., Yao, T.D., Yang, X.X., Joswiak, D.R., 2013. Implications of variations in $\delta^{18}O$ and δD in precipitation at Madoi in the eastern Tibetan Plateau. Quat. Int. 313-314, 56–61.

Rozanski, K., Araguás-Araguás, L., Gonfiantini, R., 1992. Relation between long-term trends of oxygen-18 isotope composition of precipitation and climate. Science 258 (5084), 981–985.

Rozanski, K., Araguás-Araguás, L., Giofiantini, R., 1993. Isotopic patterns in modern global precipitation. Geophys. Monogr 78, 1–36.

Salamalikis, V., Argiriou, A.A., Dotsika, E., 2015. Stable isotopic composition of atmospheric water vapor in Patras, Greece: a concentration weighted trajectory approach. Atmos. Res 152, 93–104.

Srivastava, R., Micanovic, R., El-Achkar, T.M., Janga, S.C., 2014. An intricate network of conserved DNA upstream motifs and associated transcription factors regulate the expression of uromodulin gene. Rajneesh Srivastava 192, 981–989.

Stewart, M.K., 1975. Stable isotope fractionation due to evaporation and isotopic exchange of falling water drops: applications to atmospheric processes and evaporation of lakes. J. Geophys. Res 80, 1133–1146.

Sun, C.J., Chen, Y.N., Li, W.H., Li, X.G., Yang, Y.H., 2015. Isotopic time-series partitioning of streamflow components under regional climate change in the Urumqi River, northwest China. Hydrol. Sci. J http://dx.doi.org/10.1080/02626667.2015.1031757.

Tian, L.D., Yao, T.D., Numaguti, A., 2001. Relation between stable isotope in monsoon precipitation in south Tibetan Plateau and moisture transport history. Sci. China Ser. D Earth Sci 44 (Suppl), 267–273.

Tian, L., Yao, T., MacClune, K., White, Schilla, J.W.C.A., Vaughn, B., Vachon, R., Ichiyanag, K., 2007. Stable isotopic variations in west China: a consideration of moisture sources. J. Geophys. Res 112, 3–5. http://dx.doi.org/10.1029/2006JD007718.

Vodila, G., Palcsu, L., Futo, I., Szanto, Z., 2011. A 9-year record of stable isotope ratios of precipitation in eastern Hungary: implications on isotope hydrology and regional palaeoclimatology. J. Hydrol 400, 144–153.

Wang, N., Zhang, S., Pu, J., 2008. Seasonal variation of $\delta^{18}O$ in river water in the upper reaches of Heihe River basin and its influence factors. J. Glaciol. Geocryol 30 (6), 914–920 In Chinese.

Wang, X.Y., Li, Z.Q., Edwards, R., Ruozihan, T., Zhou, P., 2016. Characteristics of water isotopes and hydrograph separation during the spring flood period in Yushugou River basin, eastern Tianshans, China. J. Earth Syst. Sci 124 (1), 115–124.

Wu, J.K., Ding, Y.J., Ye, B.S., 2010. Spatio-temporal variation of stable isotopes in precipitation in the Heihe River basin, northwestern China. Environ. Earth Sci 61, 1123–1134.

Xie, L.H., Wei, G.J., Deng, W.F., 2011. Daily $\delta^{18}O$ and δD of precipitations from 2007 to 2009 in Guangzhou, South China: implications for changes of moisture sources. J. Hydrol 400, 477–489.

Yang, Q., Xiao, H., Zhao, L., 2011a. Hydrological and isotopic characterization of river water, groundwater, and groundwater recharge in the Heihe River basin, northwestern China. Hydrol. Process 25 (8), 1271–1283.

Yang, Y.G., Xiao, H.L., Wei, Y.P., Zhao, L.J., Zou, S.B., Yin, Z.L., Yang, Q., 2011b. Hydrologic processes in the different landscape zones of Mafengou River basin in the alpine cold region during the melting period. J. Hydrol 409, 149–156.

You, Q.L., Min, J.Z., Fraedrich, K., Kang, S.C., Zhu, X.H., 2014. Projected trends in mean, maximum, and minimum surface temperature in China from simulations. Glob. Planet. Chang 112, 53–63.

You, Q.L., Min, J.Z., Lin, H.B., Kang, S.C., Pepin, N., 2015a. Observed climatology and trend in relative humidity in the eastern and central Tibetan Plateau. J. Geophys. Res. Atmos 120 (9), 3610–3621.

You, Q.L., Min, J.Z., Zhang, W., Pepin, N., Kang, S.C., 2015b. Comparison of multiple datasets with gridded precipitation observations over the Tibetan Plateau. Clim. Dyn 45, 791–806.

Yu, W., Yao, T., Lewis, S., Tian, L., Ma, Y., Xu, B., Qu, D., 2013. Stable oxygen isotope differences between the areas to the north and south of Qinling Mountains in China reveal different moisture sources. Int. J. Climatol 34, 1760–1771.

Yu, W.S., Wei, F.L., Ma, Y.M., Liu, W.J., Zhang, Y.Y., Luo, L., Tian, L.D., Xu, B.Q., Qu, D.M., 2016. Stable isotope variations in precipitation over Deqin on the southeastern margin of the Tibetan Plateau during different seasons related to various meteorological factors and moisture sources. Atmos. Res 170, 123–130.

Zhai, Y.Z., Wang, J.S., Zhang, Y., Teng, Y.G., Zuo, R., Huan, H., 2013. Hydrochemical and isotopic investigation of atmospheric precipitation in Beijing, China. Sci. Total Environ 456-457, 202–211.

Zhang, Y.H., Wu, Y.Q., 2007. Characteristics of the $\delta^{18}O$ in precipitation in the upper and middle reaches of Heihe River. J. Glaciol. Geocryol 29 (3), 440–445 In Chinese with English abstract.

Zhang, W., An, Y.H., Han, S.B., 2009. Research on the hydrogeology and stable isotope characteristics in Zhangye Plain. Ground Water 31 (6), 123–125 In Chinese.

Zhao, L.J., Yin, L., Xiao, H.L., 2011. Isotopic evidence for the moisture origin and composition of surface runoff in the headwaters of the Heihe River basin. Chin. Sci. Bull 56 (4–5), 406–415.

Zhou, S., Nakawo, M., Sakai, A., Matsuda, Y., Duan, K., Pu, J., 2007. Water isotope variations in the snow pack and summer precipitation at July 1 Glacier, Qilian Mountains in northwest China. Chin. Sci. Bull 52 (21), 2963–2972.

Zhou, W.F., Xiao, H.B., Sun, A.P., 2012. The relation between orographic cloud and vertical wind in Qilian. J. Mt. Sci 30 (6), 641–647 In Chinese.

Zhou, J.X., Wu, J.K., Liu, S.W., Zeng, G.X., Jia, Q., Wang, X.N., Zhao, Q.D., 2015. Hydrograph separation in the headwaters of the Shule River basin: combining water chemistry and stable isotopes. Adv. Meteorol 1–10, 830306.